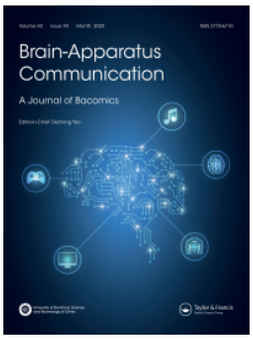

Brain-Apparatus Communication: A Journal of Bacomics

ISSN: (Print) (Online) Journal homepage: www.tandfonline.com/journals/tbac20

Limited value of a common spatial patterns approach to online discrimination of left- and right-hand motor imagery in a pediatric sample

Sarah Catherine House, Silvia Orlandi & Tom Chau

To cite this article: Sarah Catherine House, Silvia Orlandi & Tom Chau (2024) Limited value of a common spatial patterns approach to online discrimination of left- and right-hand motor imagery in a pediatric sample, Brain-Apparatus Communication: A Journal of Bacomics, 3:1, 2425299, DOI: 10.1080/27706710.2024.2425299

To link to this article: https://doi.org/10.1080/27706710.2024.2425299

Published online: 13 Nov 2024.

BRAIN-APPARATUS COMMUNICATION: A JOURNAL OF BACOMICS
2024, VOL. 3, NO. 1, 2425299
https://doi.org/10.1080/27706710.2024.2425299

Taylor & Francis
Taylor & Francis Group

RESEARCH ARTICLE

OPEN ACCESS Check for updates

Limited value of a common spatial patterns approach to online discrimination of left- and right-hand motor imagery in a pediatric sample

Sarah Catherine House[a,b], Silvia Orlandi[c] and Tom Chau[a,b]

[a]Bloorview Research Institute, Holland Bloorview Kids Rehabilitation Hospital, Toronto, Canada; [b]Institute of Biomedical Engineering, University of Toronto, Toronto, Canada; [c]Department of Electrical, Electronic, and Information Engineering – Guglielmo Marconi (DEI), University of Bologna Viale Risorgimento, Bologna, Italy

ABSTRACT

Background: Applications of brain-computer interfaces (BCIs) in pediatric rehabilitation are expanding. However, it is unclear whether popular BCI paradigms developed for adults are feasible in children. This study evaluated, in a typically developing pediatric sample, a time-honored, adult, motor imagery BCI paradigm that discriminates between imagined left- and right-hand movements.

Methods: We developed an electroencephalographic pediatric BCI with visual-auditory feedback through a game interface controlled by left- and right-hand motor imagery (MI). The BCI was evaluated in one offline (with sham feedback) and four online (with real-time classifier feedback) sessions with 11 typically developing children aged 9–14 years. The BCI was personalized to each child, *via* a well-established adult pipeline, namely, a regularized linear discriminant classifier with selected common spatial patterns in mu and beta bands as inputs.

Results: Unlike in adults, the online child-specific BCI demonstrated limited discrimination between left and right-hand MI using spatial features (52 ± 9%). Only left-hand MI versus rest in a retrospective analysis with personalized feature sets reached 70 ± 3%.

Conclusions: Our findings suggest that cortical activity corresponding to MI in our pediatric sample departed from well-documented, conspicuously lateralized adult patterns. Further investigation of developmental MI patterns is warranted to identify a pediatric approach to MI BCI.

ARTICLE HISTORY Received 6 October 2023; Accepted 30 October 2024

KEYWORDS Brain-computer interface; motor imagery; pediatric; electroencephalography; access technology

CONTACT Tom Chau tom.chau@utoronto.ca Bloorview Research Institute, Holland Bloorview Kids Rehabilitation Hospital, Toronto, ON M4G 1R8, Canada

1. Introduction

There are many conditions such as cerebral palsy, stroke, nemaline myopathy, demyelinating leukodystrophies, or cerebral malformation that compromise children's ability to communicate [1]. Brain computer interfaces (BCIs) can facilitate communication strictly by brain activity. Motor imagery (MI) is a commonly investigated mental task for BCI-based control in adults. The task involves the mental rehearsal of movement of different body parts, in the absence of actual physical movement. It is well established in adults that during movement preparation and execution, sensorimotor rhythms (SMR) momentarily attenuate (event-related desynchronization; ERD) in the associated homuncular regions of the sensorimotor cortex [2], followed by a recovery (event-related synchronization; ERS). The ERD is believed to indicate the preparation of movement and the communication between thalamocortical regions associated with motor planning [3]. In adults, these ERDs and ERSs are most prominent in mu (7–13 Hz) and beta (13–30 Hz) frequency bands in the sensorimotor cortex contralateral to the movement [4]. Topographic and spectral characteristics of these brain activities during MI are similar to, but less prominent than in actual movement [5]. Additionally, the observation of another person performing movements also elicits a similar desynchronization in mu and beta frequency bands [6].

High performance accuracies have been achieved in a variety of MI-based BCI paradigms in adults including three-dimensional control of a virtual helicopter [7] and single-channel differentiation of 4-classes of imagined movements [8]. However, thus far, nearly all MI-BCI studies have recruited adult participants. The emerging pediatric evidence is summarized below.

Jongsma et al. observed no changes in contralateral mu power (i.e. no evidence of contralateral desynchronization) but rather ipsilateral mu power increases (suggestive of inhibition) in the sensorimotor cortices accompanying imagined dominant hand movement (pointing task) in 45 typically developing children (6–12 years of age) [9]. A few studies have investigated MI BCIs with typically developing children. For example, Zhang et al. reported a range of Cohen's kappa scores from 0.025 to 0.90 for online classification of imagined hand opening and closing in 26 typically developing children (6–18 years of age) [10]. More recently, Keough et al. achieved 61% BCI training accuracy, precision and recall in classifying imagined left and right hand squeezes with 32 typically developing children (aged 6–16 years) [11]. Further elaboration on the current state of pediatric BCIs can be found in Orlandi et al. [12]. It remains unclear how well adult motor imagery BCI paradigms translate to children.

Given the dramatic differences in attention, interests, and neurophysiology between adults and children, mental tasks suitable for adults may not be appropriate for pediatric users. MI has been investigated as a promising neurorehabilitation technique in motor relearning and associated skill reacquisition in children with cerebral palsy [13], who have exhibited explicit MI skills on par with those of typically developing children. This led us to hypothesize that MI may be viable for pediatric BCIs. The goal of this study was therefore to create and evaluate an MI-driven pediatric EEG-BCI, considering a variety of MI-related features known to be robustly discriminatory in adult EEG data.

2. Methods

2.1. Participants

Thirteen typically developing, BCI-naive children were recruited and provided written informed consent. Two children had difficulty remaining still during the MI phase of the first session and did not continue with the study. Eleven participants (5 female) between the ages of 9–14 years (mean 11.5 ± 2.1 years) completed the study. Eight participants were right-handed. See Table 1. Participants had normal or corrected-to-normal vision and no history of neurologic or psychiatric conditions. All participants completed 5 sessions on separate days: 1 offline and 4 online. One participant repeated session 2 due to data contamination with excessive muscular artifacts. The experimental protocol was approved by the Research Ethics Board of Holland Bloorview Kids Rehabilitation Hospital.

2.2. Instrumentation

EEG scalp recordings were collected using active wet electrodes configured in 54–58 cm circumference caps according to the International 10–20 system [14]. Fifteen electrodes were placed on the scalp over motor-associated

Table 1. Summary of participant characteristics.

Participant	Age	Sex	Handedness
1	13	M	L
2	9	M	R
3	14	F	R
4	9	F	R
5	9	F	R
6	10	F	R
7	13	M	L
8	14	M	L
9	10	M	R
10	13	M	R
11	12	F	R

Abbreviations: M = male; F = female; L = left; R = right.

regions of the cortex (Figure 1). The ground electrode was placed at AFz, and two electrodes (TP9 and TP10) were used to create a virtual mastoid channel against which all other channels were referenced. EEG data were acquired using the BrainAmp DC amplifier (Brain Products GmbH, Germany) at a rate of 1000 Hz, with electrode impedances maintained below 25 kΩ.

Two tri-axial accelerometers (Freescale MMA7361L) were fastened on each hand using medical tape, over the distal phalange of the thumb and lumbrical muscle of the index finger, to confirm that actual muscle contractions did not occur during MI trials. Mechanomyography was selected over electromyography as the former is more sensitive to low force contractions [15]. Participants sat comfortably in a chair located approximately 80 cm from a 22" LED computer monitor with a resolution of 1680 × 1080 pixels. Figure 1 depicts the experimental setup.

2.3. Tasks

Each session comprised four tasks (see Figure 2). EEG data were collected only during movement practice and motor imagery tasks.

Meditation: To calm the participants and bring their attention to their breath, different body parts, and bodily sensations, a five-minute guided audio meditation (5-Minute Kids Body Scan Meditation) [16] was presented.

Movement Observation: Given the evidence of shared cortical activation between movement perception and action [6], participants watched for approximately 2 min, an adult performed 5 left and 5 right-hand trials (6 s each) of repeated grasping movements from a coronal view, i.e. seated behind the adult. This allocentric perspective preserved laterality, i.e. the left-side of the individual corresponded to the participant's left-side.

Movement Practice – Participants practiced 5 left and 5 right-hand grasping movement trials for approximately 2 min. The participants were

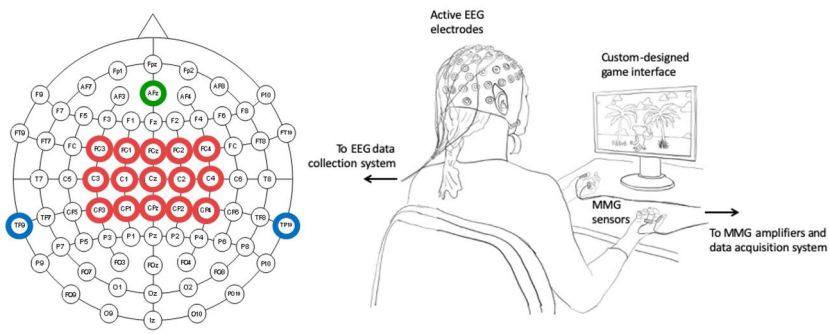

Figure 1. Instrumentation setup showing electroencephalography electrode montage on left and experimental setup on right. Abbreviations: EEG = electroencephalography; MMG = mechanomyography.

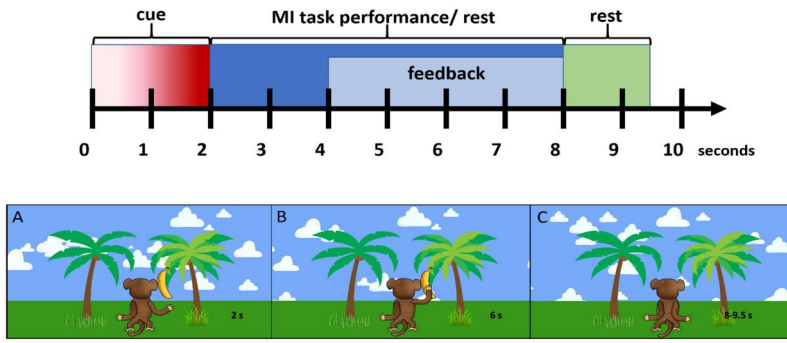

Figure 2. Session structure. The preparatory phase was common between offline and online sessions. Each run consisted of 12 motor imagery (MI) trials (5 right-hand, 5 left-hand, and 2 rest trials), in pseudorandom order. The classifier was retrained at the end of each online run with all data accumulated up to that time point.

cued by an animated monkey (on the computer screen) who raised one arm at a time, over a duration of 6 s. During this time, EEG data were collected as a reference pattern for subsequent qualitative comparison to MI trials. Participants were asked to remain as still as possible and focus on the sensations in their hands.

Motor Imagery – Participants were taught the difference between kinesthetic and visual MI and were instructed to perform the former by focusing on the sensations they experienced during the movement practice trials. They imagined left and right-hand grasping movements and were instructed to avoid actual movements. This part of the session was approximately 20 min.

2.4. Graphical interface

During movement practice and MI tasks, participants received, *via* a custom-made computer game, visual and auditory feedback, which is necessary for procedural and skill motor learning [17]. The character of the game was a stationary monkey who collected items (e.g. bananas) from its surroundings. The monkey was situated in the center of the screen facing away from the participant. A rest trial, during which the participant refrained from performing motor tasks, was indicated by a spiked ball. In an MI/movement trial, one of five translucent objects (banana, bus token, snake, snowflake, fish) faded into view (1 s) on one side of the monkey, signifying the target side for the task. The object then became opaque from bottom to top (1 s), cueing the participant to prepare for the task. The participant then performed the cued task for 6 s. During online trials, feedback (movement of one of the monkey's arms) was provided after 2 s of performing an MI task and continually updated until the end of the

trial. During movement and offline trials, errorless sham feedback was provided for the full 6 s. The participant then rested for 1.5 s.

During offline rest trials, both limbs of the monkey remained lowered. Additionally, positive auditory feedback (computer synthesized "yum" sound) was provided at the end of the 6 s of a movement or successful MI task. Trial timing and feedback are depicted in Figure 3.

2.5. Session structure

Each participant completed one offline session, where 120 trials (50 for each side, 20 for rest in pseudo random order with no more than 4 consecutive repetitions of the same MI task) were acquired to train a right vs. left MI BCI for subsequent online sessions. Between each run, the participant took a break of self-determined duration. After every two runs, the scene of the game changed to maintain participant engagement.

Four online sessions per participant were subsequently conducted with real-time feedback. The MI component of online sessions consisted of only 8 runs of 12 trials (5 left, 5 right, 2 rest). The previously trained BCI classifier was presented with new incoming EEG data and predicted the MI task. The side and extent of movement of the monkey's arm was determined by, respectively, the binary output of the classifier and the associated posterior probability (>0.7 corresponded to a maximum height of arm raise; between 0.5 and 0.7 yielded a proportionally lesser movement; <0.5 produced no movement). Correspondingly, the feedback was updated (i.e. arm moved up or down or remained stationary) every 500 ms. Successive windows of EEG data increasing in length by 500 ms

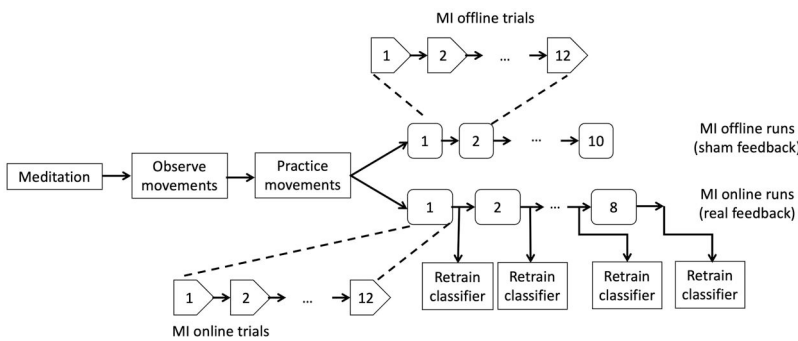

Figure 3. Timing diagram (top) of each motor imagery (MI) and movement trial. During online trials, feedback was initiated after 2 s of performing the MI task or rest. Sample feedback (bottom). (A) The beginning of a MI/movement trial. The task cue (banana) has appeared, and the monkey's arm is beginning to rise. (B) End of a trial. The monkey's arm has reached its maximum height and collects the banana. (C) The time between trials where the participant is waiting for the next task cue to appear.

increments, up to 6 s in duration, were classified. A MI trial was deemed successful if classification of the full 6 s of MI was correct and the classifier's posterior probability exceeded 0.7. At the end of each run, the classifier was retrained with all the accumulated trials. Each online session was approximately 1 h in duration. The structure of both offline and online sessions is summarized in Figure 2.

At the beginning of each session, participants rated their level of fatigue and comfort while wearing the EEG equipment. At the end of each session, participants were surveyed about post-session fatigue, frustration, focus, EEG equipment comfort, and user experience.

2.6. BCI processing pipeline

EEG signals were down sampled to 256 Hz, high pass filtered (7 Hz cut-off) and low pass filtered (30 Hz cut-off) *via* 6th order Butterworth filters. Trials were epoched from 2 to 8 s from trial onset. With the offline data (50 left-hand and 50 right-hand MI trials), features (spectral and spatial) and classifiers [18–20] commonly employed in adult MI EEG BCIs were tested. These classifiers included regularized linear discriminant analysis (LDA; with regularization parameter values of 0.1–0.6), quadratic discriminant analysis (QDA), and support vector machine (SVM; linear & Gaussian kernels with medium (3) and coarse (11) kernel scales), using 10×5-fold cross-validation. A common spatial pattern (CSP) matrix was estimated across channels for each of the mu and beta bands. The EEG data in each band were projected onto their corresponding reduced CSP matrix comprising 2 eigenvectors. The log of the variance of each dimension of the CSP-projected EEG [21], along with mu (7–12 Hz) band power (P_{μ}), and beta (13–30 Hz) band power (P_{β}) of each channel were extracted as features. The feature set dimensionality was reduced to 15 using the ReliefF feature selection algorithm [22], which has been widely deployed in motor imagery BCI design [23,24]. The most accurate feature set-classifier combination was selected for the online session. Between online sessions, the classifier hyperparameters were re-optimized for each participant. Sessional BCI classification accuracy was determined as the proportion of correctly classified trials among the final 40 trials. The first 40 trials were treated as same-day training data. All chance levels were estimated using the binomial distribution, considering the number of trials and an $\alpha = 0.05$ [25].

2.7. Retrospective analyses

In the retrospective analysis, we tested different variations of features and classifiers. An alternative filter bank (FB) to the one used online was also

investigated; 6 different frequency bands of signal, namely, 4–8 Hz, 8–12 Hz, 12–16 Hz, 16–20 Hz, 20–24 Hz, and 24–28 Hz were extracted. Data from all 5 sessions were pooled (210 left-hand, 210 right-hand MI trials, 84 rest trials). In addition to the log of the variance of the CSP-projected EEG (using 2 eigenvectors for the CSP projection for each band) and μ and β power, the following additional features were extracted per channel: fractal dimension (D), estimated using both Higuchi's ($k_{max} = 8$) and Katz's methods [26], and trial-averaged instantaneous frequencies (f) and energy (E) [27] estimated by empirical mode decomposition followed by the Hilbert-Huang transform [28]. For left vs. right-hand MI classification, 10×5-fold cross-validation was performed with 10 feature sets: {log-variance CSP}, {log-variance CSP_{FB}},{P_{μ}, P_{β}}, {P_{FB}}, {D}, {D_{FB}},{f}, {f_{FB}}, {E}, {E_{FB}}, where the subscript FB denotes the filter bank mentioned above and {log-variance CSP} refers to the log of the variance of the retained dimensions of the CSP-projected EEG. For MI vs. rest classification, thirteen feature sets were tested:{log-variance CSP},{log-variance CSP_{FB}},{P_{μ}, P_{β}},{P_{FB}}, {D},{D_{FB}},{f}, {f_{FB}}, {E}, {E_{FB}}, {CSP_{FB}, P_{FB}}, {P_{FB}, D_{FB}}, and {CSP_{FB}, P_{FB}, D_{FB}}. Features that achieved the highest average classification accuracy across participants and exceeding 60%, were then tested in combination with other features. Features were reduced to a subset of 15 using the RelieFf algorithm. The same classifiers as above were tested. For classification between MI and rest, MI trials were randomly subsampled to match the total number of rest trials ($n = 84$). Classification accuracies were compared by a Friedman non-parametric test as the feature distributions violated normality (Shapiro-Wilk test for normality).

To visually contrast the ERS and ERD during the MI trials against the signal activity of rest trials, spectrograms were created (with a sliding window of 125 samples, where successive windows overlapped by 100 samples). ERD and ERS were identified by a trial-averaged, negative or positive change in relative power [29], respectively,

$$\Delta PSD^{L} = \frac{PSD^{L}_{task} - PSD_{rest}}{PSD_{rest}} \times 100\% \quad (1)$$

where PSD^{L}_{task} denotes the PSD (power spectral density) during a left MI task and PSD_{rest} is the PSD of the rest signal, and $\Delta PSD^{L} < 0$ indicates an ERD. The relative power change on the right side, ΔPSD^{R}, was defined similarly. The PSD in the mu frequency band was averaged for each channel and plotted topographically since studies with adults report most prominent lateralization in the mu band [30].

3. Results

3.1. Session 1: Offline

For seven participants (P1-P4, P6, P8, P9) accuracies did not exceed chance levels (58.0%) using any of the tested features for left vs. right-hand MI classification. Accuracies exceeded chance for all features for P11 and with at least one feature for P5, P7 and P10. Across participants, the average classification accuracies using a regularized LDA classifier with optimized γ parameter were: $55 \pm 6.8\%$ for log-variance CSP features, $56 \pm 5.2\%$ for P_{μ} features, $52 \pm 5.0\%$ for P_{β} features, and $55 \pm 7.2\%$ for their combination. There were no differences in average accuracies among the features or across classifiers (Friedman test; $p > 0.05$). Given this finding and considering computational efficiency, log-variance CSP features with a regularized LDA were thus selected for the online sessions.

3.2. Sessions 2–5: Online

As seen in Figure 4, only 4 participants exceeded the chance level in at least one online session (participants 4, 5, 10, and 11) for left vs. right MI classification. The average accuracy achieved by participants was $52 \pm 9\%$. The maximum achieved accuracy in one session was 78% (P4 in session 3). No trend was observed between sessions. MMG data were visually inspected during the sessions to identify movement during the MI trials. No MI trials were removed.

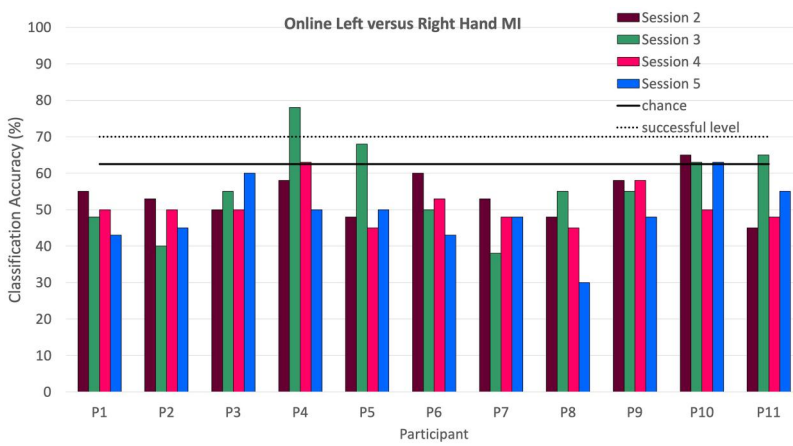

Figure 4. Online classification accuracies for left versus right-hand motor imagery (MI) using common spatial pattern features during sessions 2–5, based on the final 40 trials in each session. Chance level was 62.5% ($p < 0.05$) according to the binomial distribution with $n = 40$ test trials.

3.3. Subjective ratings

Most participants (10) rated the EEG cap as comfortable, the ease of imagining single hand movement as somewhat strenuous and fatigue as increased after at least one of the five sessions. The ease of understanding their performance was rated between somewhat strenuous to difficult by nine and easy by two participants. Most participants (7) noted their initial ability to focus as facile but reported difficulty in focusing by session end. Most participants reported a high level of enjoyment combined with some level of frustration and boredom.

3.4. Retrospective analysis

For left vs. right hand MI, retrospective classification accuracies did not exceed chance (54.0%; $n = 420$, $p > 0.05$) for 3 participants (P1, P4, P9) with any of the tested features. For the remaining participants, the feature sets yielding above-chance accuracies varied. Considering only the feature set with the highest accuracy for each participant, an average classification accuracy of $57 \pm 4\%$ was achieved retrospectively. On average, no feature set yielded accuracies exceeding 60%.

For MI vs. rest classification using 15 log-variance CSP features, retrospective classification exceeded the chance level of 56.5% ($p < 0.05$, $n = 168$) for 9 participants. The average classification accuracies across participants for left-hand MI versus rest ($60 \pm 4\%$) and right-hand MI versus rest ($60 \pm 3\%$) were not significantly different (Wilcoxon signed-rank test, $p > 0.05$). For both classification problems, band power features from the filter bank, P_{FB}, yielded the highest classification accuracy (exceeding 60%) in 10 participants and significantly exceeded accuracies attained with other features (Friedman test and post-hoc pairwise comparison with Tukey-Kramer correction; $p \ll 0.05$). An average classification accuracy of $70 \pm 3\%$ was obtained for left-hand MI vs. rest when considering only the highest accuracy feature set per participant.

3.5. Topographic plots

The topographic plots of P6, P8, and P10 (right hand only), and P11 are shown in the right column of Figure 5. These participants exhibited a strong ERD (−50%) over the hand region of the sensorimotor cortex (C3 and C4), and ERS in surrounding cortical areas during actual movement. P2, P4, and P10 (left hand only) exhibited some ERD but also some atypical ERS patterns. The left column of Figure 5 depicts the topographic plots of the same participants during MI. Surprisingly, there was little evidence of ERD during MI for any of the participants. P4, P6, and P10

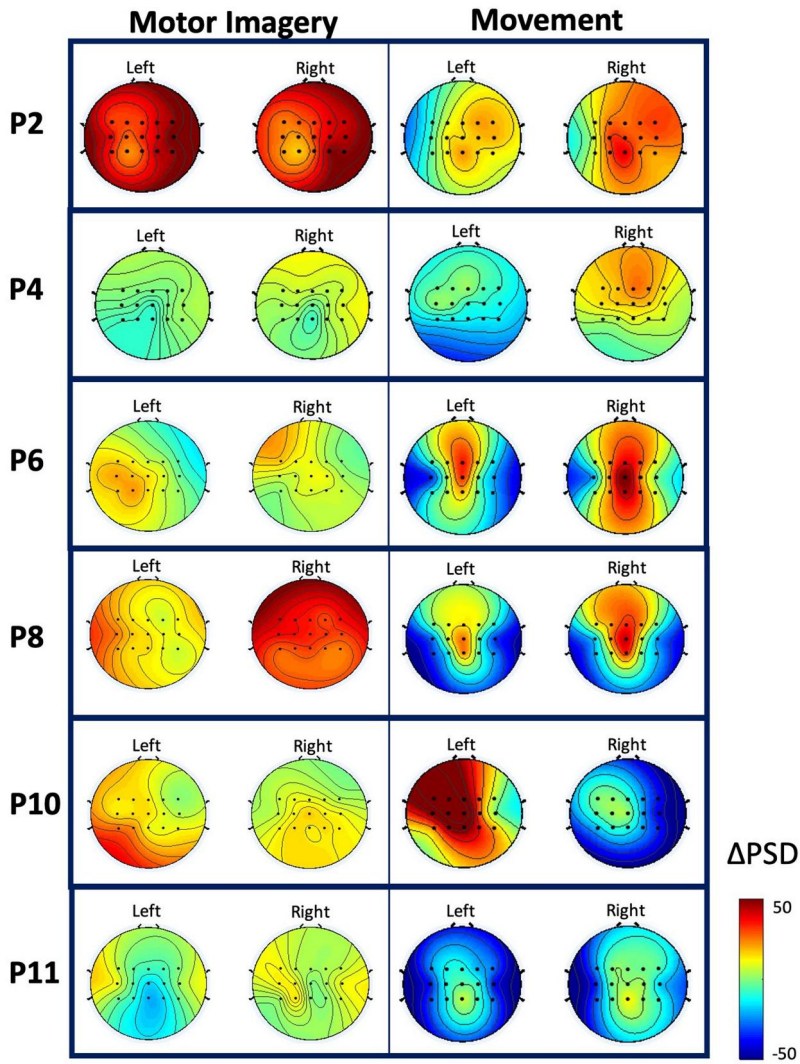

Figure 5. Topographic plots of event-related synchronization and event-related desynchronization (from retrospective analysis) for participants P1 through P11. Power band activity was averaged across all motor imagery (MI) trials and across 10 movement trials. Color bar depicts relative change in power spectral density (ΔPSD).

demonstrated modest ERD in the contralateral hemispheres. P2 and P8 had an overall pattern of synchronization which is typically not associated with MI. P11 exhibited a reversed pattern with ERS in electrodes over the hand region of the sensorimotor cortex (C3 and C4) and ERD in surrounding regions.

4. Discussion

4.1. Discrimination between left and right-hand motor imagery

Online left vs. right hand MI classification accuracies suggest that time-honored CSP-based feature, i.e. logarithm of the variances of the first and last CSP eigenvectors deployed in adult studies were not discernible in our pediatric sample regardless of the machine learning algorithm. This finding contradicts the lateralization observed when many of the participants performed actual movement (Figure 5). No trend among online sessional accuracies was observed (Figure 4). Overall, the online BCI using log-variance CSP features did not provide the pediatric participants with successful control of the on-screen monkey. This finding was unexpected as studies with adults have generated high accuracies with CSP [8] and band power features [31]. However, our findings seem to be supported by Jongsma et al. [9] who observed that typically developing children only exhibited contralateral desynchronization dominance during motor execution and not when performing hand motor imagery.

4.2. Motor imagery vs. rest classification

The accuracies achieved in our sample were low even for MI vs. rest classification given that adult EEG MI-BCI studies involving up to four classes have attained much greater accuracies [7,8,32]. The limited accuracies were in part attributable to the high intra-individual variation in EEG signals, indicated by the large SD among the iterations of cross-validation (average 8% classification accuracy across participants). Further, as ERD/ERS estimates depended on rest trial data, spurious brain activity during rest (e.g. participant engages in a mental task) would have compromised the detection of SMR modulations.

4.3. Contextualizing within the pediatric EEG BCI literature

To the best of the authors' knowledge, only four studies have reported performance of an MI EEG BCI with pediatric participants [10,11,33,34]. Three studies [10,33,34] utilized a commercially available EMOTIV EPOC® or EPOC+® EEG headset and preprogrammed BCI software for analysis and classification. As a result, none of these studies evaluated specific feature sets for classification. Zhang et al. [10] recruited typically developing children (6–18 years), while Jadavji et al. [34] and Taherian et al. [33] recruited children with perinatal stroke and spastic quadriplegic cerebral palsy, respectively. Zhang et al. [10] reported age-dependent but modest overall performance among participants with a mean Cohen's kappa of 0.403 (SD = 0.277) when

classifying MI versus baseline, which is comparable to the average classification accuracy achieved in our left-hand MI versus rest classification (70 ± 3%) with slightly younger (9–14 years) participants. Additionally, Zhang et al. [10] employed a backward counting task as the neutral state. Differentiating between two active tasks often yields higher accuracies than the discrimination between an active task and unconstrained rest [35], as in our study. Lastly, Zhang et al. [10] considered a trial as correct if any degree of task activation was detected in the first 8 s of their 20 s trial, whereas in our study, a successful MI trial required sustained MI activation over the duration of the 6 s trial and accurate classification of the entire trial at its conclusion. Keough et al. [11] collected data from 32 typically developing children using a 24-channel dry headset. They used the tangent space projection of covariance matrices estimated over 2 s windows as feature vectors for logistic regression-based classification of left- and right-hand MI. Only training (not testing) metrics were provided with mean accuracy, precision and recall at 0.61 (0.57–0.65 95% confidence interval), which are comparable to our online test results. It thus appears that our findings corroborate the modest classification accuracies achieved thus far in other MI BCI studies with typically developing children.

4.4. Pediatric considerations for motor imagery EEG BCI

Children generally have shorter attention spans than adults and BCI performance is known to improve with heightened concentration [36]. The drift in mental state associated with the self-reported onset of fatigue and difficulty with focusing likely altered EEG activity during MI trials, partially contributing to the signal variation among trials. Additionally, psychological factors such as perceived task difficulty and fatigue reported by our participants, are known to alter BCI performance in adults [37] and may be even more pronounced in children.

The MI topographic plots in Figure 5 clearly deviate from patterns typically generated in adult EEG-MI studies [38]. While some participants exhibited a maximum ERD of −50% in hand representations of the sensorimotor cortex, adult participants have frequently demonstrated much larger ERDs (e.g. up to −100% ERD [39]). Our findings seem to indicate that children in the 9–14-year age range tend to produce attenuated ERDs compared to those of adults during an MI task.

ERD/ERS patterns are known to vary among adult participants in terms of magnitude [39] and dominant frequency components [38]. Similarly, the topographic plots (Figure 5) of actual movement in the present study varied across participants in terms of strength and presence of ERD/ERS. However, our findings suggest that variation in MI-related

brain activity appears to be more extensive in children than in adults. Pediatric-specific variation in ERD/ERS may be attributed to neurodevelopmental stage of motor, prefrontal executive control, and attention systems [40]. The cortical area producing mu and beta band activity associated with motor movement increases by 10–15 cm^2 during childhood [41]. Axons in major fiber pathways develop through childhood and into adulthood, entailing significant myelination [42] and synaptic pruning of excitatory contacts [43]. EEG activity created by developing brains has been shown to yield differences in both resting [44] and movement-related [45] frequency dynamics. Children may also approach a simple mental task with a greater diversity of cognitive strategies than adults, which may decrease the consistency of EEG dynamics [46]. These neurophysiological and neurocognitive differences between adult and children likely contributed to the observed variability in MI-BCI performance.

4.5. Limitations

Children may be more prone to perform visual rather than kinesthetic MI, which might explain the lack of strong ERD in motor hand representations. Visual MI is known to predominantly activate occipital regions of the brain in adults [47]. During online trials, participants frequently received incongruent feedback (the monkey's hand opposite to the side of MI was raised) whenever classification of left versus right-hand MI was incorrect. This incongruent feedback was intended to promote motor learning. However, it is possible although unlikely (since offline trials with congruent feedback also yielded low accuracies), that an observation-related desynchronization was induced in the contralateral sensorimotor cortex, diminishing any lateralization of activity due to the MI task. Finally, although most electrode impedances fell far below 20 kΩ throughout data collection, there were occasional occurrences over the 5 sessions where channel impedances escalated beyond this level. These aberrations may have increased low frequency noise in the locally recorded signal [48] and contributed to obfuscation of any underlying desynchronization. However, the input amplifier's high input impedance likely had a mitigating effect.

4.6. Future work

To improve classification accuracy of pediatric EEG signals accompanying motor imagery, future studies may depart from conventional CSP to consider time-frequency-spatial patterns [49] or various deep learning architectures recently proposed for motor imagery EEG BCIs [50]. These

approaches may be better suited to modelling the dynamic and highly variable nature of pediatric MI brain signals within and between sessions. Another future direction may be to investigate hybrid pediatric BCIs where the classifier is provided multiple data sources such as EEG and electro-ocular signals to leverage natural movements accompanying motor imagery [51]. Finally, motor imagery training [52] may help children to produce more repeatable and discernible MI brain signals. As participant feedback provided insight into task difficulty, future studies should continue to capture subjective experiences of pediatric BCI users.

5. Conclusion

We evaluated personalized MI-driven EEG-BCIs with a pediatric sample ($N = 11$) both online and *via* retrospective analyses. The BCIs did not reliably classify left versus right-hand MI using log-variance CSP features in online gamified sessions. Retrospective offline discrimination between a single MI task and rest, using personalized feature sets (beyond CSP) reached $70 \pm 3\%$ across participants. Attenuated or absent ERD/ERS while performing MI tasks in our sample suggest deviation from the familiar strongly lateralized patterns observed in adults. As such, robustly discriminatory EEG signal features in adults were not useful in the machine classification of MI in our pediatric sample.

Disclosure statement

No potential conflict of interest was reported by the author(s).

Funding

This work was supported in part by the Natural Sciences and Engineering Research Council of Canada [RGPIN-2019-06033].

Notes on contributors

Sarah Catherine House has an interest in brain-computer interfaces and their application for children with neurodevelopmental disabilities. She completed a Master of Applied Science in Biomedical Engineering in 2018 and Doctor of Medicine in 2024, both at the University of Toronto. She employed electroencephalography to investigate motor imagery-driven brain-computer interfaces in the pediatric population. She worked as a research coordinator supporting the launch of a new pediatric clinical brain-computer interface program at Holland Bloorview Kids Rehabilitation Hospital in Toronto, Canada.

Silvia Orlandi earned her Ph.D. in 2015 from the Department of Electrical, Electronic, and Information Engineering—Guglielmo Marconi (DEI) at the

University of Bologna. Following her doctoral studies, she completed post-doctoral fellowships at the Department of Information Engineering, University of Firenze, Italy, and the Bloorview Research Institute, Holland Bloorview Kids Rehabilitation Hospital, Toronto, Canada. Currently, she serves as an Assistant Professor at DEI, University of Bologna, Italy. Her research is centered on speech science and the development of human-machine interfaces that aid in the diagnosis of neurodevelopmental disorders and neurorehabilitation therapies for individuals with cognitive and motor impairments. Her work encompasses a wide range of technologies, including virtual reality, brain-computer interfaces, and wearable devices. She is committed to advancing the field of assistive technology to enhance the lives of those facing neurological challenges.

Tom Chau is a Professor in the Institute of Biomedical Engineering and Distinguished Senior Scientist at Holland Bloorview Kids Rehabilitation Hospital. He holds the Raymond G. Chang Foundation Chair in Access Innovations. His research focuses on the investigation of novel access pathways to facilitate communication for children and youth with severe physical impairments. Chau's lab has developed numerous access innovations that are being used by children and youth, locally and abroad, including: The Virtual Music Instrument, a computer vision-based software tool that allows children of all abilities to play music and a vocal fold vibration device that enables communication by humming. His lab has created a variety of optical, ultrasonic, and electrical brain-computer interfaces (BCIs) that facilitate communication and control through mental activities. These innovations helped to introduce BCIs to the pediatric clinical setting in 2013.

ORCID

Sarah Catherine House http://orcid.org/0000-0001-7051-2827
Silvia Orlandi http://orcid.org/0000-0003-2733-8450
Tom Chau http://orcid.org/0000-0002-7486-0316

References

1 Vos RC, Dallmeijer AJ, Verhoef M, et al. Developmental trajectories of receptive and expressive communication in children and young adults with cerebral palsy. Dev Med Child Neurol. 2014;56(10):951–959. doi:10.1111/dmcn.12473.
2 Moghimi S, Kushki A, Marie Guerguerian A, et al. A review of EEG-based brain-computer interfaces as access pathways for individuals with severe disabilities. Assist Technol. 2013;25(2):99–110. doi:10.1080/10400435.2012.723298.
3 Pangelinan MM, Kagerer FA, Momen B, et al. Electrocortical dynamics reflect age-related differences in movement kinematics among children and adults. Cereb Cortex. 2011;21(4):737–747. doi:10.1093/cercor/bhq162.
4 Bamdad M, Zarshenas H, Auais MA. Application of BCI systems in neurorehabilitation: a scoping review. Disabil Rehabil Assist Technol. 2015;10(5):355–364. doi:10.3109/17483107.2014.961569.
5 Schalk G, Miller KJ, Anderson NR, et al. Two-dimensional movement control using electrocorticographic signals in humans. J Neural Eng. 2008;5(1):75–84. doi:10.1088/1741-2560/5/1/008.

6 Aridan N, Ossmy O, Buaron B, et al. Suppression of EEG mu rhythm during action observation corresponds with subsequent changes in behavior. Brain Res. 2018;1691:55–63. doi:10.1016/j.brainres.2018.04.013.
7 Doud AJ, Lucas JP, Pisansky MT, et al. Continuous three-dimensional control of a virtual helicopter using a motor imagery based brain-computer interface. PLoS One. 2011;6(10):e26322. doi:10.1371/journal.pone.0026322.
8 Ge S, Wang R, Yu D. Classification of four-class motor imagery employing single-channel electroencephalography. PLoS One. 2014;9(6):e98019. doi:10.1371/journal.pone.0098019.
9 Jongsma MLA, Steenbergen B, Baas CM, et al. Lateralized EEG mu power during action observation and motor imagery in typically developing children and children with unilateral Cerebral Palsy. Clin Neurophysiol. 2020;131(12):2829–2840. doi:10.1016/j.clinph.2020.08.022.
10 Zhang J, Jadavji Z, Zewdie E, et al. Evaluating if children can use simple brain computer interfaces. Front Hum Neurosci. 2019;13:24. doi:10.3389/fnhum.2019.00024.
11 Keough J, Irvine B, Kelly D, et al. Fatigue in children using motor imagery and P300 brain-computer interfaces. J Neuroeng Rehab. 2024;21(1):61. doi:10.1186/s12984-024-01349-2.
12 Orlandi S, House SC, Karlsson P, et al. Brain-computer interfaces for children with complex communication needs and limited mobility: a systematic review. Front Hum Neurosci. 2021;15:643294. doi:10.3389/fnhum.2021.643294.
13 Cabral-Sequeira AS, Coelho DB, Teixeira LA. Motor imagery training promotes motor learning in adolescents with cerebral palsy: comparison between left and right hemiparesis. Exp Brain Res. 2016;234(6):1515–1524. doi:10.1007/s00221-016-4554-3.
14 Homan RW, Herman J, Purdy P. Cerebral location of international 10-20 system electrode placement. Electroencephalogr Clin Neurophysiol. 1987;66(4):376–382. doi:10.1016/0013-4694(87)90206-9.
15 Alves N, Chau T. The design and testing of a novel mechanomyogram-driven switch controlled by small eyebrow movements. J Neuroeng Rehab. 2010;7[cited:22. Oct 30];7. doi:10.1186/1743-0003-7-22.
16 5-Minute Kids Body Scan Meditation w/Cory Muscara [Internet]. 2017. [cited 2024 Jun 25]. Available from: https://www.youtube.com/watch?v=u3Jmy74UKcs.
17 Galea JM, Mallia E, Rothwell J, et al. The dissociable effects of punishment and reward on motor learning. Nat Publ Group. 2015;18(4):597–602.
18 Fu R, Tian Y, Bao T, et al. Improvement motor imagery EEG classification based on regularized linear discriminant analysis. J Med Syst. 2019;43(6):169. doi:10.1007/s10916-019-1270-0.
19 Lotte F, Guan C, Ang KK. Comparison of designs towards a subject-independent brain-computer interface based on motor imagery. 2009 Annual International Conference of the IEEE Engineering in Medicine and Biology Society [Internet]. 2009. [cited 2024 Oct 18]. p. 4543–4546. Available from: https://ieeexplore.ieee.org/abstract/document/5334126. doi:10.1109/IEMBS.2009.5334126.
20 Ma Y, Ding X, She Q, et al. Classification of motor imagery EEG signals with support vector machines and particle swarm optimization. Comput

Math Methods Med. 2016;2016(1):4941235–4941238. doi:10.1155/2016/4941235.
21 Yu Y, Zhou Z, Liu Y, et al. Self-paced operation of a wheelchair based on a hybrid brain-computer interface combining motor imagery and P300 potential. IEEE Trans Neural Syst Rehabil Eng. 2017;25(12):2516–2526. doi:10.1109/TNSRE.2017.2766365.
22 Kononenko I. Estimating attributes: analysis and extensions of RELIEF. In: Bergadano F, Raedt L, editors. Machine learning: ECML 1994. Lecture Notes in Computer Science. Berlin, Heidelberg: Springer; 1994. p. 171–182.
23 Ramos AC, Hernández RG, Vellasco M. Feature selection methods applied to motor imagery task classification. 2016 IEEE Latin American Conference on Computational Intelligence (LA-CCI) [Internet]. 2016. [cited 2024 Oct 18]. p. 1–6. Available from: https://ieeexplore.ieee.org/abstract/document/7885731. doi:10.1109/LA-CCI.2016.7885731.
24 Koprinska I. Feature selection for brain-computer interfaces. Theeramunkong T, Nattee C, Adeodato PJL, et al., editors. New frontiers in applied data mining. Berlin, Heidelberg: Springer; 2010. p. 106–117.
25 Combrisson E, Jerbi K. Exceeding chance level by chance: the caveat of theoretical chance levels in brain signal classification and statistical assessment of decoding accuracy. J Neurosci Methods. 2015;250:126–136. doi:10.1016/j.jneumeth.2015.01.010.
26 Güçlü U, Güçlütürk Y, Loo CK. Evaluation of fractal dimension estimation methods for feature extraction in motor imagery based brain computer interface. Procedia Comput Sci. 2011;3:589–594. doi:10.1016/j.procs.2010.12.098.
27 Jerbic AB, Horki P, Sovilj S, et al. Hilbert-Huang time-frequency analysis of motor imagery EEG data for brain-computer interfaces. 6th European Conference of the International Federation for Medical and Biological Engineering; 2015. p. 62–63.
28 Huang NE, Shen SSP. Hilbert–Huang transform and its applications. Interdisciplinary mathematical sciences. Vol. 16. Singapore: World Scientific; 2014.
29 Nguyen NQ, Truong QDK, Kondo T. Fractals properties of EEG during event-related desynchronization of motor imagery. Proc Annu Int Conf IEEE Eng Med Biol Soc. 2015:2015:4146–4149.
30 McFarland DJ, Miner LA, Vaughan TM. et al. Mu and Beta Rhythm Topographies During Motor Imagery and Actual Movements. Brain Topogr. 2000;12:177–186. doi:10.1023/A:1023437823106.
31 Zaky MH, Khedr ME, Nasser AA. Effect of extensive training load on the classification accuracy for a three class motor imagery based brain-computer interface. 2016 3rd International Conference on Advances in Computational Tools for Engineering Applications (ACTEA). 2016. p. 211–215.
32 LaFleur K, Cassady K, Doud A, et al. Quadcopter control in three-dimensional space using a noninvasive motor imagery-based brain–computer interface. J Neural Eng. 2013;10(4):046003. doi:10.1088/1741-2560/10/4/046003.
33 Taherian S, Selitskiy D, Pau J, et al. Training to use a commercial brain-computer interface as access technology: a case study. Disabil Rehabil Assist Technol. 2016;11(4):345–350. doi:10.3109/17483107.2014.967313.

34 Jadavji Z, Zhang J, Paffrath B, et al. Can children with perinatal stroke use a simple brain computer interface? Stroke. 2021;52(7):2363–2370. doi:10.1161/STROKEAHA.120.030596.

35 C Schudlo L, Chau T. Towards a ternary NIRS-BCI: single-trial classification of verbal fluency task, Stroop task and unconstrained rest. J Neural Eng. 2015;12(6):066008. doi:10.1088/1741-2560/12/6/066008.

36 Mahmoudi B, Erfanian A. Electro-encephalogram based brain–computer interface: improved performance by mental practice and concentration skills. Med Biol Eng Comput. 2006;44(11):959–969. doi:10.1007/s11517-006-0111-8.

37 Myrden A, Chau T. A passive EEG-BCI for single-trial detection of changes in mental state. IEEE Trans Neural Syst Rehabil Eng. 2017;25(4):345–356. doi:10.1109/TNSRE.2016.2641956.

38 Neuper C, Scherer R, Reiner M, et al. Imagery of motor actions: differential effects of kinesthetic and visual–motor mode of imagery in single-trial EEG. Brain Res Cogn Brain Res. 2005;25(3):668–677. doi:10.1016/j.cogbrainres.2005.08.014.

39 Höller Y, Bergmann J, Kronbichler M, et al. Real movement vs. motor imagery in healthy subjects. Int J Psychophysiol. 2013;87(1):35–41. doi:10.1016/j.ijpsycho.2012.10.015.

40 Bender S, Weisbrod M, Bornfleth H, et al. How do children prepare to react? Imaging maturation of motor preparation and stimulus anticipation by late contingent negative variation. NeuroImage. 2005;27(4):737–752. doi:10.1016/j.neuroimage.2005.05.020.

41 Roland J, Miller K, Freudenburg Z, et al. The effect of age on human motor electrocorticographic signals and implications for brain–computer interface applications. J Neural Eng. 2011;8(4):046013. doi:10.1088/1741-2560/8/4/046013.

42 Tang E, Giusti C, Baum GL, et al. Developmental increases in white matter network controllability support a growing diversity of brain dynamics. Nat Commun. 2017;8(1):1252. doi:10.1038/s41467-017-01254-4.

43 Selemon LD. A role for synaptic plasticity in the adolescent development of executive function. Transl Psychiatry. 2013;3(3):e238–e238. doi:10.1038/tp.2013.7.

44 Matsuura M, Yamamoto K, Fukuzawa H, et al. Age development and sex differences of various EEG elements in healthy children and adults—quantification by a computerized wave form recognition method. Electroencephalogr Clin Neurophysiol. 1985;60(5):394–406. doi:10.1016/0013-4694(85)91013-2.

45 Thorpe SG, Cannon EN, Fox NA. Spectral and source structural development of mu and alpha rhythms from infancy through adulthood. Clin Neurophysiol. 2016;127(1):254–269. doi:10.1016/j.clinph.2015.03.004.

46 Segalowitz SJ, Santesso DL, Jetha MK. Electrophysiological changes during adolescence: a review. Brain Cogn. 2010;72(1):86–100. doi:10.1016/j.bandc.2009.10.003.

47 Guillot A, Collet C, Nguyen VA, et al. Brain activity during visual versus kinesthetic imagery: an fMRI study. Hum Brain Mapp. 2009;30(7):2157–2172. doi:10.1002/hbm.20658.

48 Kappenman ES, Luck SJ. The Effects of electrode impedance on data quality and statistical significance in ERP recordings. Psychophysiology. 2010;47(5):888–904. doi:10.1111/j.1469-8986.2010.01009.x.

49 Miao Y, Jin J, Daly I, et al. Learning common time-frequency-spatial patterns for motor imagery classification. IEEE Trans Neural Syst Rehabil Eng. 2021;29:699–707. doi:10.1109/TNSRE.2021.3071140.

50 Altaheri H, Muhammad G, Alsulaiman M, et al. Deep learning techniques for classification of electroencephalogram (EEG) motor imagery (MI) signals: a review. Neural Comput & Applic. 2023;35(20):14681–14722. doi:10.1007/s00521-021-06352-5.

51 Hosni SM, Shedeed HA, Mabrouk MS, et al. EEG-EOG based virtual keyboard: toward hybrid brain computer interface. Neuroinform. 2019;17(3):323–341. doi:10.1007/s12021-018-9402-0.

52 Behrendt F, Zumbrunnen V, Brem L, et al. Effect of motor imagery training on motor learning in children and adolescents: a systematic review and meta-analysis. Int J Environ Res Public Health. 2021;18(18):9467. doi:10.3390/ijerph18189467.